

Synthesis, Topological Analysis and Properties of a Coordination Polymer with Butane-1,2,3,4-tetracarboxylato-bridged (Phenanthroline)cobalt(II) Units

Hong-Lin Zhu and Yue-Qing Zheng

State Key Laboratory Base of Novel Functional Materials & Preparation Science, Center of Applied Solid State Chemistry Research, Ningbo University, Ningbo, 315211, P. R. China

Reprint requests to Prof. Dr. Yue-Qing Zheng. Fax: Int. +574/87600747.

E-mail: zhengcm@nbu.edu.cn

Z. Naturforsch. **2011**, *66b*, 119–124; received October 27, 2010

A hydrothermal reaction of $\text{Co}(\text{Ac})_2 \cdot 4\text{H}_2\text{O}$, butane-1,2,3,4-tetracarboxylic acid (H_4BTC), 1,10-phenanthroline (phen) and NaOH carried out at 160 °C yielded a new complex $[\text{Co}_2(\text{H}_2\text{O})_2(\text{phen})_2(\text{BTC})]$. The complex has been characterized by single-crystal X-ray diffraction, IR spectroscopy, TG-DTA analyses, elemental analyses, powder X-ray diffraction, and magnetic measurements. The Co ions are linked by BTC^{4-} anions into a chain, and hydrogen bonding and π - π stacking interactions result in the formation of a 3D (3,4,6)-connected supramolecular architecture with the Schläfli symbol $(4^3.6^2.8)_2(4^6.6^6.8^3)(6^3)_2$. The temperature dependence of the magnetic susceptibility of the compound follows a Curie-Weiss law $\chi_m = C/(T - \Theta)$ with $C = 4.18(4) \text{ cm}^3 \text{ mol}^{-1} \text{ K}$ and $\Theta = -1.43(5) \text{ K}$, and the magnetic behavior can be interpreted by means of a 1D chain Fisher model, where the magnetic superexchange is transmitted via $\pi \cdots \pi$ stacking interactions between adjacent phen ligands, and the best fit results in $J = -0.05 \text{ cm}^{-1}$, and $zJ' = 0.21 \text{ cm}^{-1}$.

Key words: Supramolecular Architecture, Butane-1,2,3,4-tetracarboxylic Acid, Crystal Structure, Topology, Magnetic Properties

Introduction

Supramolecular systems have attracted great attention in recent years due to their potential as functional materials as well as their intriguing structural topologies [1–4]. It is well known that supramolecular assemblies can be designed and constructed based on non-covalent intermolecular interactions such as hydrogen bonds, aromatic $\pi \cdots \pi$ stacking, electrostatic and van der Waals forces, and hydrophobic and hydrophilic interactions. In particular, hydrogen bonds and aromatic $\pi \cdots \pi$ stacking interactions play important roles in supramolecular architectures [5–7]. No doubt, multi-carboxylic acids and heteroaromatic *N*-donor ligands such as 1,10-phenanthroline and 2,2-bipyridine have become the ideal candidates for the rational design and synthesis of such materials [7–9].

The past decade has witnessed an expansion of research on supramolecular architectures such as adamantane-, benzene and pyridine-based carboxylic acid and flexible α, ω -dicarboxylic acids [10–14].

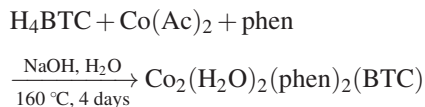
In contrast, utilization of aliphatic multi-carboxylic acids seems relatively limited in the construction of supramolecular architectures [15–18]. Out of the series of aliphatic multi-carboxylic acids, butane-1,2,3,4-tetracarboxylic acid (H_4BTC) is of special interest. The H_4BTC molecule possesses four ionizable protons that can be removed gradually. When two of these protons are removed the $\text{H}_2\text{BTC}^{2-}$ ligand is generated which is found in $[\text{Y}_2(\text{H}_2\text{O})_6(\text{H}_2\text{BTC})(\text{BTC})] \cdot 5\text{H}_2\text{O}$ [19], and when all four protons are removed, the resulting ligand can bridge metal atoms to form a series of coordination polymers [19–23]. The Co atoms in $[\text{Co}(\text{bbi})(\text{BTC})_{1/2}] \cdot \text{H}_2\text{O}$ (bbi = 1,1'-(1,4-butanediyl)-bis(imidazole)) are bridged by BTC^{4-} anions to form layers, which are interconnected by bbi to form 3D α -Po topological frameworks [20]. As a part of our ongoing systematic investigation of aliphatic multi-carboxylic acid complexes, we report a new butane-1,2,3,4-tetracarboxylato-bridged cobalt(II) complex $[\text{Co}_2(\text{H}_2\text{O})_2(\text{phen})_2(\text{BTC})]$.

Results and Discussion

Syntheses

Reaction of $\text{Co}(\text{Ac})_2 \cdot 4\text{H}_2\text{O}$, butane-1,2,3,4-tetracarboxylic acid, 1,10-phenanthroline and NaOH under hydrothermal conditions at 160 °C afforded the title compound. Repeated experiments have shown that the synthesis of the title compound is also successful at 140 °C, but the yields are lower. On the other hand, reactions carried out at 180 °C yielded only an unidentifiable mixture. This implies that the most suitable temperature for the syntheses of the title compound

is 160 °C. The optimized conditions are expressed in terms of the following equation:



The powder XRD pattern of the compound matches well with that simulated on the basis of the single crystal data (Fig. 1). The title compound is found to be stable in air and insoluble in common solvents such as water, ethanol and methanol.

Description of the crystal structure

The asymmetric unit of the title compound consists of one Co^{2+} cation, one 1,10-phenanthroline, half a butane-1,2,3,4-tetracarboxylate tetraanion and one aqua ligand as shown in Fig. 2. The crystallographically centrosymmetric BTC^{4-} ion is centered at the Wyckoff site 1*f*. Each carboxylate group monoatomically coordinates to one metal atom, functioning as a $\mu_4\eta^4$ bridging ligand. Compared to free 1,10-phenanthroline, the present chelating phen ligand preserves its nearly perfect coplanarity. The Co atoms are each coordinated by two N atoms from one phen ligand, two oxygen atoms from two BTC ligands and one aqua ligand to complete a CoN_2O_3 core. The Co-N/O contact distances range from 2.015(3) to 2.199(3) Å, and the N/O–Co–N/O angles are in the region 76.3–163.6(1)°. The above bonding characteristics of the Co atoms are all within the normal ranges [24, 25]. The Addison τ value of 0.61 ($\tau = 0$ for an ideal square pyramid and

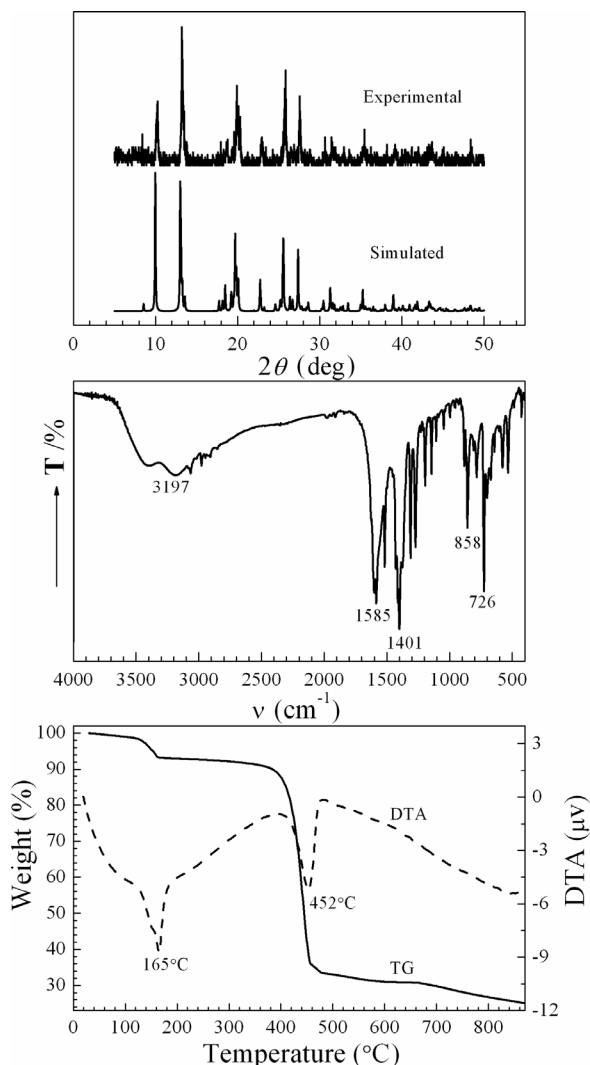


Fig. 1. Experimental and simulated PXRD patterns (top), infrared spectrum (middle), and TG-DTA curves for **1** (bottom).

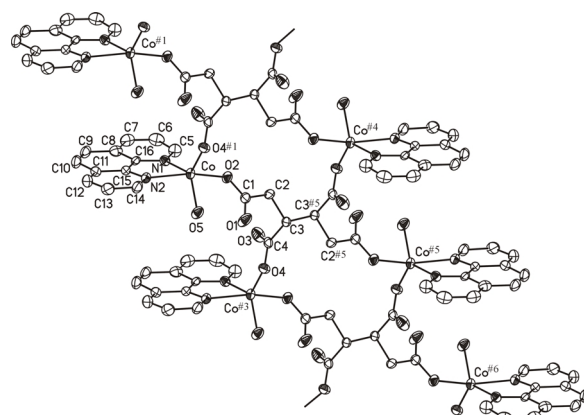


Fig. 2. ORTEP view of a fragment of the polymeric chains $[\text{Co}_2(\text{H}_2\text{O})_2(\text{phen})_2(\text{BTC})_{4/4}]$ with displacement ellipsoids (45 % probability) and atomic labeling.

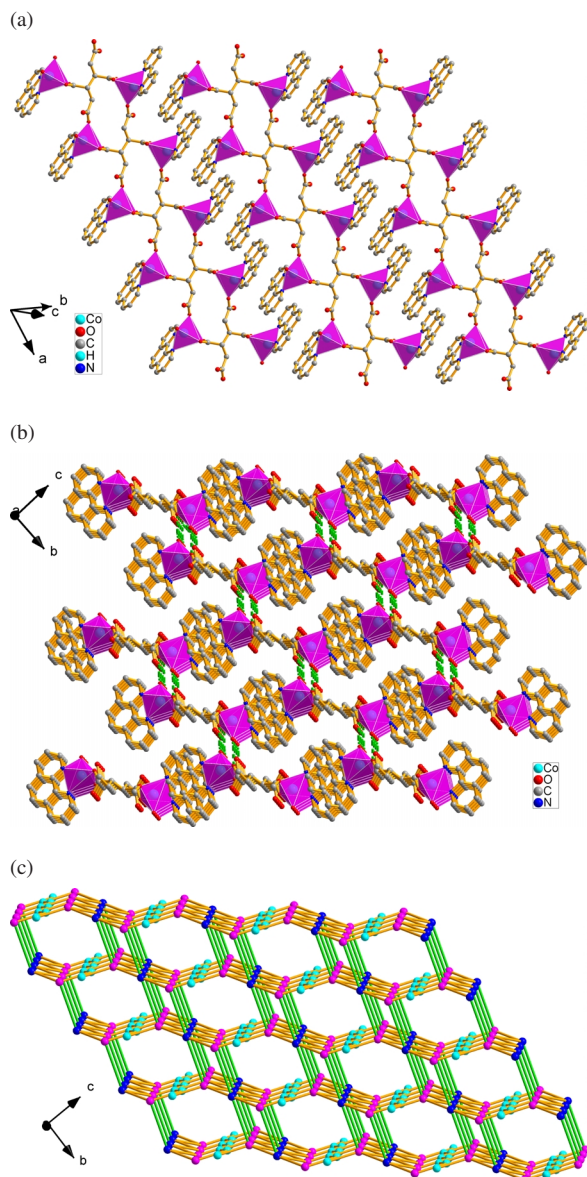


Fig. 3. (a) Supramolecular assembly of layers through $\pi \cdots \pi$ stacking interactions; (b) supramolecular assembly of the layers into a 3D architecture based on hydrogen bonds; (c) the topological representation of the 3D architecture in crystals of **1**.

$\tau = 1$ for an ideal trigonal bipyramid) indicates that the CoN_2O_3 core is intermediate between the two ideal geometries [26].

The penta-coordinated Co atoms are bridged by BTC^{4-} anions to form ribbons extending infinitely along the [100] direction, to be formulated as $\frac{1}{\infty}[\text{Co}_2(\text{H}_2\text{O})_2(\text{phen})_2(\text{BTC})_{4/4}]$ with the phen ligands

orientated outwards. The mean interplanar distances of the 1,10-phenanthroline ligands between adjacent chains are 3.25 and 3.44 Å, indicating significant intermolecular $\pi \cdots \pi$ stacking interactions, which are regarded as the driving forces to generate supramolecular layers parallel to (011) as demonstrated in Fig. 3a. Each layer is shifted by $\frac{1}{2}(\vec{c} + \vec{b})$ with respect to the adjacent neighbor, and along the [011] axis the layers are stacked in an $\cdots \text{ABAB} \cdots$ sequence. The aqua ligand donates one hydrogen atom to the carboxylate oxygen atom O1 to form intrachain hydrogen bonds with $d(\text{O}-\text{H} \cdots \text{O}) = 2.574$ Å and $\angle(\text{O}-\text{H} \cdots \text{O}) = 160^\circ$, and provides another hydrogen atom to the carboxylate oxygen atom O4^{#2} to form an interlayer hydrogen bond with $d(\text{O}-\text{H} \cdots \text{O}) = 2.715$ Å and $\angle(\text{O}-\text{H} \cdots \text{O}) = 173^\circ$. No doubt, the intrachain hydrogen bonding interactions contribute to the stabilization of the chain, and the interlayer hydrogen bonding interactions are responsible for the assembly of the layers into a 3D supramolecular architecture (Fig. 3b).

If from the viewpoint of network topology, the interchain $\pi \cdots \pi$ stacking interactions and interlayer hydrogen bonding interactions are taken into account, the 1,10-phenanthroline ligands are each three-connected to one Co atom as well as to two neighboring 1,10-phenanthroline molecules *via* $\pi \cdots \pi$ stacking interactions with a vertex symbol of (6.6.6). Each Co atom can be treated as four-connected linking three BTC^{4-} anions and one 1,10-phenanthroline with a vertex symbol of (4.6.4.6.4.8₆), and each BTC^{4-} anion is six-connected to six Co atoms with a vertex symbol of (4.4.4.4.4.6₂.6₂.6₂.6₂.6₃.6₃.8₈.8₁₀.8₁₀). Thus, the 3D supramolecular architecture can be topologically described as a 3-D (3,4,6)-connected network with the Schläfli symbol of $(4^3.6^2.8)_2(4^6.6^6.8^3)(6^3)_2$ as illustrated in Fig 3c.

Infrared spectrum

The IR spectrum of **1** (Fig. 1) shows a broad band centered at 3197 cm^{-1} , which is diagnostic of the water molecules. The asymmetric vibrations (ν_{as}) of the carboxylate groups result in a strong absorption band at 1585 cm^{-1} , while the medium-strong absorption due to the symmetric vibrations (ν_{s}) is observed at 1312 cm^{-1} . The wavenumber difference of 273 cm^{-1} suggests that the carboxylate groups is in a monodentate coordination mode [27]. The sharp absorption peaks observed at 1401, 3065 and 726 cm^{-1} can be ascribed to the pyridyl ring and

to C-H deformation vibrations. From a comparison with butane-1,2,3,4-tetracarboxylic acid, the weak absorptions at 2910 and 1280 cm^{-1} can be attributed to out-of-plane C-H bending vibrations and the O-C-C stretching vibrations of the butane-1,2,3,4-tetracarboxylate anions.

Thermal analysis

The thermal behavior of the title compound is depicted in Fig. 1. The DTA curve shows two strong endothermic peaks at 165 and 452 $^{\circ}\text{C}$. The observed weight loss for the first step over 100–180 $^{\circ}\text{C}$ reaches 5.8%, close to the calculated value (4.84%) for the loss of two water molecules per formula unit. The dehydration thus leads to the formation of an anhydrous intermediate “ $\text{Co}_2(\text{phen})_2(\text{BTC})$ ”. The second step between 350–500 $^{\circ}\text{C}$ can be attributed to the decomposition of the butane-1,2,3,4-tetracarboxylate ligand and a release of the 1,10-phenanthroline ligand. When further heated, the resulting intermediate loses weight very slowly over 500–870 $^{\circ}\text{C}$, and the observed weight loss of 8.0% corresponds well to the value of 7.53% calculated for 2 equivalents of “CO”. The dark residue left at 870 $^{\circ}\text{C}$ represents 25.04% in weight.

Magnetic properties

The magnetic properties of the title compound in the form of $\chi_m T$ and χ_m^{-1} vs. T plots (the molar magnetic susceptibility per Co_2 unit) at a magnetic field of 5 kOe are represented in Fig. 4. For the title compound, the effective $\chi_m T$ value for the Co^{2+} ions at r. t. is 4.87 $\text{cm}^3 \text{mol}^{-1} \text{K}$, which is much

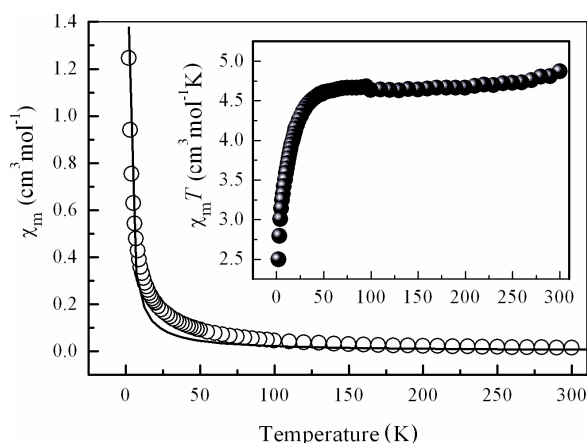


Fig. 4. Temperature dependence of the magnetic susceptibilities. Solid lines represent the best fit.

larger than the spin-only value of 3.75 $\text{cm}^3 \text{mol}^{-1} \text{K}$ for high-spin $\text{Co}(\text{II})$ ($S = 3/2$), but corresponds to common values for high-spin $\text{Co}(\text{II})$ centers (4.63–6.77) [28]. Upon cooling, the $\chi_m T$ value gradually decreases to 4.61 $\text{cm}^3 \text{K mol}^{-1}$ at 50 K, then abruptly diminishes to 2.50 $\text{cm}^3 \text{K mol}^{-1}$ at 2 K, which is typical of overall antiferromagnetic interactions between $\text{Co}(\text{II})$ ions. The χ_m can be fit to the Curie-Weiss equation ($\chi_m = C/T - \Theta$) with the Curie constant $C = 4.18(4) \text{ cm}^3 \text{mol}^{-1} \text{K}$ and a Weiss constant of $\Theta = -1.43(5) \text{ K}$, indicating weak antiferromagnetic interactions between the $\text{Co}(\text{II})$ ions. The above structure description shows that the effective transmitting pathway of the magnetic coupling between the magnetic centers may be the significant $\pi \cdots \pi$ interactions between adjacent chelating phen ligands. Therefore, the magnetic structure can be modeled for a chain via $\pi \cdots \pi$ interactions with the Hamiltonian as $H = -J \sum_{i,j} \hat{S}_i \hat{S}_j$, and the Fisher model for an infinite chain of identical $S = 3/2$ spins with an isotropic J coupling constant (Eqs. 1 and 2) [29, 30]. Owing to the very weak magnetic interactions between ions, the expression is corrected using the molecular field approximation (Eq. 3), to which the magnetic susceptibility data were fitted.

$$\chi'_m = \frac{N\beta g^2}{3kT} S(S+1) \frac{(1+u)}{(1-u)} \quad (1)$$

$$u = \coth \left(\frac{2JS(S+1)}{KT} \right) - \left(\frac{2JS(S+1)}{KT} \right)^{-1} \quad (2)$$

$$\chi_m = \frac{\chi'_m}{1 - (2zJ/Ng^2\beta^2)\chi'_m} \quad (3)$$

S is the spin moment ($S = 3/2$), and J represents the coupling constant between two $\text{Co}(\text{II})$ ions linked by $\pi \cdots \pi$ interactions. The best fit is obtained with values of $g = 2.19$, $J = -0.05 \text{ cm}^{-1}$, $zJ = 0.21 \text{ cm}^{-1}$, and $R = 5.4 \times 10^{-3}$ ($R = \sum [(\chi_m)_{\text{obs}} - (\chi_m)_{\text{calc}}]^2 / [(\chi_m)_{\text{obs}}]^2$), where the negative J value indicates a very weak ferromagnetic coupling between the $\text{Co}(\text{II})$ ions, and the positive zJ' clearly indicates the existence of the antiferromagnetic coupling between adjacent $\text{Co}(\text{II})$ ions, consistent with the magnetic behavior illustrated by the $\chi_m T$ vs. T plot.

Conclusion

A new butane-1,2,3,4-tetracarboxylate $\text{Co}(\text{II})$ compound $\text{Co}_2(\text{H}_2\text{O})_2(\text{phen})_2(\text{BTC})$ has been obtained

from a hydrothermal reaction. The Co atoms are linked by BTC⁴⁻ anions into a chain $\frac{1}{\infty}[\text{Co}_2(\text{H}_2\text{O})_2(\text{phen})_2(\text{BTC})_4/4]$, and hydrogen bonding interactions and $\pi \cdots \pi$ stacking interactions are responsible for the assembly of a 3D supramolecular network corresponding to the Schläfli symbol of $(4^3.6^2.8)_2(4^6.6^6.8^3)(6^3)_2$. The magnetic characterization suggests weak antiferromagnetic coupling exchange *via* $\pi \cdots \pi$ stacking interactions, and the best fit results for $J = -0.05 \text{ cm}^{-1}$, $zJ' = 0.21 \text{ cm}^{-1}$.

Experimental Section

Materials

All chemicals of reagent grade were commercially available and used without further purification.

Physical methods

Powder X-ray diffraction measurements were carried out with a Bruker D8 Focus X-ray diffractometer to check the phase purity. C, H and N microanalyses were performed with a PE 2400II CHNS elemental analyzer. The FT-IR spectrum was recorded from KBr pellets in the range 4000–400 cm^{-1} on a Shimadzu FTIR-8900 spectrometer. Thermogravimetric measurements were carried out from room temperature to 870 °C on preweighed samples using a Seiko Exstar 6000 TG/DTA 6300 apparatus with a heating rate of 10 °C min^{-1} . The temperature-dependent magnetic susceptibility was determined with a Quantum Design SQUID magnetometer (Model MPMS-7) in the temperature range 2–300 K with an applied field of 5 kOe.

Synthesis of $[\text{Co}_2(\text{H}_2\text{O})_2(\text{phen})_2(\text{BTC})]$

A mixture of 0.058 g (0.25 mmol) butane-1,2,3,4-tetracarboxylic acid, 0.077 g (0.50 mmol) $\text{Co}(\text{Ac})_2 \cdot 4\text{H}_2\text{O}$, 0.0988 g (0.50 mmol) 1,10-phenanthroline, 0.040 g (1.00 mmol) NaOH and water (10 mL) was sealed in a 23 mL Teflon-lined stainless-steel autoclave, which was heated to 160 °C and kept at this temperature for 4 d under autogeneous pressure. Then the reactor was allowed to cool to room temperature. Pink block-shaped crystals were collected from the Teflon liner and air-dried (yield 62% based on the initial $\text{Co}(\text{Ac})_2 \cdot 4\text{H}_2\text{O}$ input). – IR (film): $\nu = 3197, 3065, 2978, 2910, 1602, 1585, 1517, 1401, 1312, 1280, 1195, 1144, 1110, 1043, 998, 858, 783, 726, 580, 534 \text{ cm}^{-1}$. – $\text{C}_{28}\text{H}_{26}\text{Co}_2\text{N}_4\text{O}_{10}$ (744.43): calcd. C 51.63, H 3.52, N 7.53; found C 51.56, H 3.83, N 7.42.

X-Ray structure determination

Suitable single crystals were selected under a polarizing microscope and fixed with epoxy cement on fine glass fibers which were then mounted on a Rigaku R-Axis Rapid IP X-ray diffractometer operating with graphite-

Table 1. Crystal structure data for **1**.

Formula	$\text{C}_{32}\text{H}_{26}\text{Co}_2\text{N}_4\text{O}_{10}$
M_r	744.43
Cryst. size, mm^3	$0.19 \times 0.11 \times 0.05$
Crystal system	triclinic
Space group	$P\bar{1}$
$a, \text{Å}$	7.654(2)
$b, \text{Å}$	9.564(2)
$c, \text{Å}$	10.889(2)
α, deg	84.24(3)
β, deg	71.41(3)
γ, deg	67.87(3)
$V, \text{Å}^3$	699.7(2)
Z	1
$D_{\text{calcd}}, \text{g cm}^{-3}$	1.77
$\mu(\text{MoK}\alpha), \text{cm}^{-1}$	1.3
$F(000), e$	380
hkl range	$\pm 9, \pm 12, \pm 14$
$2\theta_{\text{max}}, \text{deg}$	54.9
Refl. measd / unique / R_{int}	3174 / 2229 / 0.066
Param. refined	218
$R1(F) / wR2(F^2)^a$ (all refl.)	0.0801 / 0.1532
A / B (weighting scheme) ^a	0.0649 / 0.2239
GoF (F^2) ^b	1.230
$\Delta\rho_{\text{fin}}$ (max / min), $e \text{ Å}^{-3}$	0.89 / –0.72

^a $R1 = \sum ||F_o| - |F_c|| / \sum F_o$, $wR2 = [\sum w(F_o^2 - F_c^2)^2 / \sum w(F_o^2)^2]^{1/2}$, $w = [\sigma^2(F_o^2) + (AP)^2 + BP]^{-1}$, where $P = (\text{Max}(F_o^2, 0) + 2F_c^2) / 3$ and A and B are constants adjusted by the program; ^b $\text{GoF} = S = [\sum w(F_o^2 - F_c^2)^2 / (n_{\text{obs}} - n_{\text{param}})]^{1/2}$, where n_{obs} is the number of data and n_{param} the number of refined parameters.

Table 2. Selected bond lengths (Å), and angles (deg) for **1** with estimated standard deviations in parentheses.

Distances					
Co–O2	2.015(3)	Co–N1	2.092(3)		
Co–O4 ^{#1}	2.030(3)	Co–N2	2.199(3)		
Co–O5	2.015(3)				
Angles					
O2–Co–O4 ^{#1}	101.5(1)	O4 ^{#1} –Co–N1	125.6(1)		
O2–Co–O5	91.0(1)	O4 ^{#1} –Co–N2	94.9(1)		
O2–Co–N1	93.6(1)	O5–Co–N1	131.9(1)		
O2–Co–N2	163.6(1)	O5–Co–N2	85.9(1)		
O4 ^{#1} –Co–O5	100.0(1)	N1–Co–N2	76.8(1)		
Hydrogen bonding contacts					
D–H	d(D–H)	d(H \cdots A)	d(D–H \cdots A)	$\angle(\text{D–H}\cdots\text{A})$	A
O5–H5B	0.79	1.82	2.574	160	O1
O5–H5C	0.82	1.91	2.715	173	O4 ^{#2}

monochromatized $\text{MoK}\alpha$ radiation ($\lambda = 0.71073 \text{ Å}$) for cell determination and subsequent data collection. The reflection intensities in the θ range 3.00–27.45° were collected at 293 K using the ω scan technique. The employed single crystals exhibited no detectable decay during the data collection. The data were corrected for Lp and empirical absorption effects. The programs SHELXS-97 and SHELXL-97 [31, 32] were used for structure solution and refinement. The structure was solved by using Direct Methods. Subsequent difference Fourier syntheses enabled all non-hydrogen atoms to

be located. After several cycles of refinement, all hydrogen atoms associated with carbon atoms were geometrically generated, and the rest of the hydrogen atoms were located from the successive difference Fourier syntheses. Finally, all non-hydrogen atoms were refined with anisotropic displacement parameters by full-matrix least-squares techniques, and hydrogen atoms with isotropic displacement parameters set to 1.2 times the values for the associated heavier atoms. Detailed information about the crystal data and structure determination is summarized in Table 1. Selected interatomic distances and bond angles including hydrogen bond parameters are given in Table 2.

CCDC 796245 contains the supplementary crystallographic data for this paper. These data can be obtained free of charge from The Cambridge Crystallographic Data Centre via www.ccdc.cam.ac.uk/data_request/cif.

Acknowledgement

This project was supported by the National Natural Science Foundation of China (grant No. 20072022), the Science and Technology Department of Zhejiang Province (grant No. 2006C21105), and the Education Department of Zhejiang Province. Honest thanks are also expressed for sponsoring by the K. C. Wong Magna Fund of Ningbo University.

- [1] J.-P. Zhang, X.-C. Huang, X.-M. Chen, *Chem. Soc. Rev.* **2009**, *38*, 2385–2396.
- [2] M. J. Zaworotko, *Cryst. Growth Des.* **2007**, *7*, 4–9.
- [3] N. C. Gianneschi, M. S. Masar III, C. A. Mirkin, *Acc. Chem. Res.* **2005**, *38*, 825–837.
- [4] L. Kovbasyuk, R. Kramer, *Chem. Rev.* **2004**, *104*, 3161–3187.
- [5] L. Brunsveld, B. J. B. Folmer, E. W. Meijer, R. P. Sijbesma, *Chem. Rev.* **2001**, *101*, 4071–4097.
- [6] M. C. T. Fyfe, J. F. Stoddart, *Acc. Chem. Res.* **1997**, *30*, 393–401.
- [7] D. L. Caulder, R. N. Raymond, *Acc. Chem. Res.* **1999**, *32*, 975–982.
- [8] E. C. Constable, V. Chaurin, C. E. Housecroft, M. Neuburger, S. Schaffner, *CrystEngComm* **2008**, *10*, 1063–1069.
- [9] X. Li, D.-Y. Cheng, J.-L. Lin, Z.-F. Li, Y.-Q. Zheng, *Cryst. Growth Des.* **2008**, *8*, 2853–2861.
- [10] B.-L. Chen, L.-B. Wang, F. Zapata, G.-D. Qian, E. B. Lobkovsky, *J. Am. Chem. Soc.* **2008**, *130*, 6718–6719.
- [11] Y. Wu, A. Kobayashi, G. J. Halder, V. K. Peterson, K. W. Chapman, N. Lock, P. D. Southon, C. J. Kepert, *Angew. Chem.* **2008**, *120*, 9061–9064; *Angew. Chem. Int. Ed.* **2008**, *47*, 8929–8932.
- [12] O. Fabelo, J. Pasán, F. Lioret, M. Julve, C. Ruiz-Pérez, *Inorg. Chem.* **2008**, *47*, 3568–3576.
- [13] S. K. Ghosh, G. Savitha, P. K. Bharadwaj, *Inorg. Chem.* **2004**, *43*, 5495–5497.
- [14] K. Hanson, N. Calin, D. Bugaris, M. Scancella, S. C. Sevov, *J. Am. Chem. Soc.* **2004**, *126*, 10502–10503.
- [15] Y.-Q. Zheng, J.-L. Lin, W. Xu, H.-Z. Xie, J. Sun, X.-W. Wang, *Inorg. Chem.* **2008**, *47*, 10280–10287.
- [16] A. K. Ghosh, D. Ghoshal, E. Zangrando, J. Ribas, N. R. Chaudhuri, *Inorg. Chem.* **2007**, *46*, 3057–3071.
- [17] M. S. Wang, G. C. Guo, L. Z. Cai, W. T. Chen, B. Liu, A. Q. Wu, J. S. Huang, *J. Chem. Soc., Dalton Trans.* **2004**, 2230–2236.
- [18] I. Vlahou, N. Kourkoumelis, A. Michaelides, S. Skoulika, J. C. Plakatouras, *Inorg. Chim. Acta* **2006**, *359*, 3540–3548.
- [19] H.-L. Zhu, Y.-Q. Zheng, *J. Mol. Struct.* **2010**, *970*, 27–35.
- [20] Y.-Y. Liu, J.-F. Ma, J. Yang, J.-C. Ma, Z.-M. Su, *Cryst EngComm* **2008**, *10*, 894–904.
- [21] Y. Cheng, J. Wu, H.-L. Zhu, J.-L. Lin, *Acta Crystallogr.* **2009**, *E65*, o835.
- [22] H. A. Barnes, J. C. Barnes, *Acta Crystallogr.* **1996**, *C63*, 731–736.
- [23] L. C. Delgado, O. Fabelo, J. Pasán, F. S. Delgado, F. Lloret, M. Julve, C. Ruiz-Pérez, *Inorg. Chem.* **2007**, *46*, 7458–7465.
- [24] S.-J. Fu, C.-Y. Cheng, K.-J. Lin, *Cryst. Growth Des.* **2007**, *7*, 1381–1384.
- [25] D.-C. Wen, S.-X. Liu, M. Lin, *J. Mol. Struct.* **2008**, *876*, 154–161.
- [26] A. W. Addison, N. Rao, *J. Chem. Soc., Dalton Trans.* **1984**, 1349–1356.
- [27] K. Nakamoto, *Infrared and Raman Spectra of Inorganic and Coordination Compounds*, 4th ed., Interscience-Wiley, New York, **1986**.
- [28] O. Kahn, *Molecular magnetism*, VCH Publisher, New York, **1993**.
- [29] T. D. Keene, M. B. Hursthouse, D. J. Price, *Cryst. Growth Des.* **2009**, *9*, 2604–2609.
- [30] P. Alborés, E. Rentschler, *Dalton Trans.* **2009**, 2609–2615.
- [31] G. M. Sheldrick, SHELXS-97, Program for the Solution of Crystal Structures, University of Göttingen, Göttingen (Germany) **1997**. See also: G. M. Sheldrick, *Acta Crystallogr.* **1990**, *A46*, 467–473.
- [32] G. M. Sheldrick, SHELXL-97, Program for the Refinement of Crystal Structures, University of Göttingen, Göttingen (Germany) **1997**. See also: G. M. Sheldrick, *Acta Crystallogr.* **2008**, *A64*, 112–122.